Original Article

Skin Lesion Border Detection Based on Optimal Statistical Model Using Optimized Colour Channel

Alaa Ahmed Abbas¹*, Fadeheela Sabri Abu-Almash¹

Middle Technical University, Ministry of Higher Education and Scientific Research

ABSTRACT

This paper proposes an effective way to segment melanoma skin lesion in colour dermoscopic images, using an edge-based approach. The proposed method, different methods were combined to improve the segmentation performance. These methods are morphological operations, bilateral filter, spline, polynomial model and canny edge detector. Different methods were tested to select the best method that was produced the best outcome. These testing methods, bilateral filter provided the highest PSNR amongst other filters such as median filter, Gaussian and average filter. Two statistical models were implemented polynomial model and linear regression and selected the best performance as polynomial model. Four edge detectors were applied to detect the edge of skin lesion and select the best segmentation accuracy. Manual border selection was used as the benchmark to evaluation the accuracy of the automatic border. The proposed method was able to achieve a good average accuracy of 96.69% based on canny edge detector. Our dataset consists of (70) dermoscopic images that includes melanoma and nevus.

Keywords: Bilateral Filter; Spline; Polynomial Model; Linear Regression Model; Edge Detection; Canny; Melanoma; Skin Lesion

*CORRESPONDING AUTHOR
Alaa Ahmed Abbas, Middle Technical
University, Ministry of Higher Education and
Scientific Research;
alaa.abayechi@gmail.com;

1. Introduction

Segmentation techniques are commonly used in image analysis to separate the objects from its background, so that the object isolated can be used for further examination. In computer aided medical diagnosis, segmentation is also considered as an essential step towards accurate medical analysis. Specifically when analysing medical images, segmentation methods can extract crucial medical information on anatomical structures to facilitate identification of abnormalities. In dermoscopic images, there are several characteristic features of skin lesions that enable physicians to determine whether the lesion is malignant or benign, by focusing on different features as shape, colour, size and symmetry. An accurate diagnosis of a malignant melanoma may allow the patient to find treatment and enhance his/hers likelihood for survival[1]. In general, melanoma has varied shapes, colours, and texture, it may be a challenge for an automated system to detect the entirety of the lesion.

There are many approaches for segmentation in image processing, such as thresholding, region, and edge detection. Edge detection is one of the important methods, which used in computer vision. Then, the quality of edge detection is important to low-level image processing. A good 'edge' is essential for higher level processing[2]. Edge detection was focused in this paper to separate the skin lesion area as foreground from the surrounding healthy skin as background.

(Stoecker, Gupta, Stanley, Moss, & Shrestha, 2005)Automated border

detection being one of the main focus for dermoscopic image evaluation, its reasons are twofold: firstly, the overall shape of the border provides important insights in obtaining an accurate diagnosis, this is because one of the essential characteristic differences between malignant and benign skin lesions is that malignant lesions have irregular borders, whereas benign lesions' border are considerably smoother and round; another important feature differences being extracted using automated border detection is that it is capable of extracting atypical pigment networks, called globules[3], as well as blue-white areas[4], these are some of the important signifiers of an malignant melanoma. The detection of these features critically depends on the accuracy of automated border detection.

There are a few challenges in automated border detections for lesion segmentation. The quality of edge detection is dependent upon the lighting conditions when the images were captured, while different camera settings may affect the outcome of a captured image and this could result in inconsistencies across the dataset. Some images in our dataset may have low contrast between the lesion and the surrounding skin and unwanted artefacts such as hair, air bubbles, and dates. Lesions can be different in colour, and malignant lesions sometimes have varied colours within the lesion, this heightened the difficulty in differentiating the lesion from the healthy skin. The aim of this paper is to find an optimal edge detector with good smoothing specifically for dermoscopic images. The organization of this paper is as follows: Section 2 reviews the related work and Section 3 describes the proposed segmentation algorithm. The experimental results and discussion are continued in Section 4, where section 5 presents the conclusions and suggestions for future work.

2. Related Work

Filters are useful for removing noise and is usually used in the pre-processing stage to prepare the images for further analysis. Many researchers have used various filter techniques to aid noise reduction in image processing and analysis. Tomasi[5] utilized geometric closeness and their photometric similarity for grey level and colour images, then implemented filtering on the three colour channels (R, G, and B) individually, then different values of sigma σ_d and σ_r were evaluated. They were able to reduce the phantom colour that appears in the original image. Numerous of researchers applied bilateral filter to obtain smooth images while preserving important details[6–9]. Global threshold was applied to detect border of the skin lesion and refine the border using the optimal channels from CIEXYZ colour space[11]. Yasmin and Sathik[12] compared two edge detectors, Canny and Laplacian of Gaussian filter (LoG) were used to detect border of skin lesion with good accuracy results. Wavelet and curvelet were combined by Mahmoud to detect the border of the lesion then extracted features of the lesion[14]. From the literature, it can be seen that bilateral filter is a desirable method for filter as it enables satisfactory results while preserving the edges. In this paper, an optimization of the bilateral filter is proposed to improve its performance.

Both linear regression model and polynomial model have been used by researchers to estimate variables in image analysis, linear regression was applied to fit the model with the observation variables[15]. Also, The polynomial model was used for adjusting the satellite image[16] and estimated roughness from the surface of the lesion from the dermoscopic images[17]. In addition, the linear regression was implemented by Almedeij to estimate evaporation in Kuwait[18]. The correlation coefficient was computed between evaporation and other variables for linearize the existing curvilinear patterns of the data by using power and exponential functions.

In this work, an edge-based segmentation method was adopted to identify the border of skin lesions. There have been a wide range of applications and methods using various types of edge detection technique in image processing and image analysis. A number of border detection methods have been reported in the literature[19,20]. Some methods include histogram thresholding followed by region growing[21], global threshold using optimal colour channels followed by morphological operations[23], Hybrid thresholding[24]. There different edge detectors as Sobel, Prewitt, Zero-crossing and Canny[30,37,38] were applied in different application as well as to detect edge of skin lesion[25,35] and have obtain good results.

In the next section, a flow chart of our proposed method consists of three main steps pre-processing, edge segmentation, and post processing. It is shown to provide a good illustration of the steps taken in our method.

3. Tested Techniques in the Proposed Method

In this section, we describe the experimental techniques involved in the development of the proposed method. In this case, the images were first smoothed through the application of image filter. The optimal colour channel was then selected. Next, their intensities were rescaled and smoothed with spline. The intensities of the images were estimated using a mathematical model before the skin lesions were delineated using an edge based segmentation technique. The steps involved in our method are summarized graphically by the flowchart in **Figure 1**.

3.1 Pre-processing

The images in the database were consisted of dermoscopic images from different devices such as Epi-luminescence Microscopy (ELM) and digital photographs. There was a total of 70 images in our database that contains both malignant and benign skin lesions (Melanoma). These images were originated from different sources that provided images with a varied sizes and lighting condition as well as different skin tones. This is to ensure that our results is free from any likely dependencies with a certain source of images.

3.1.1 Image resizing and noise removal

The first step in the process was to resize the image as to standardize their sizes. The images were consistently filled with noises such as date of the image, ruler for measurement, thick and thin hairs, and lighting from the flash. The second step was to remove the background noise from the images as to increase the quality of the edge detection on the images. Morphological closing and erosion were implemented to remove the thick hairs and lighting, respectively.

3.1.2 Rescaling image using Bilt-Sp

In this step, four filters which were average filter, median filter, Gaussian filter and bilateral filter to were tested to evaluate their performance in noise removal. The average filter is a linear filter that leads to a smooth image as it replaces the pixels in the image with the average of their neighbourhood. Conversely, the median filter is a nonlinear filter that replaces each pixel by the median value of the neighbourhood. The Gaussian filter is a low pass filter that explores relationships between the spatial and frequency domains. Different values of standard deviation can be used to adjust the size of the Gaussian filter's mask.

Bilateral filter is a nonlinear filter for image de-noising. A Gaussian kernel function was used for both domain and range filtering. The results were dependent on filtering and based on pixel intensity. The pixels of the domain filter, based on their distance from the centre, were computed using the following formula[8]:

$$P(x - y) = \frac{1}{2} e^{-(x-y)^2 \left(\frac{1}{2\sigma^2_D} \right)} \tag{1}$$

where x and y represent the spatial coordinates of the pixel, and σ_D is the spatial scale.

The range filter weights pixels based on tonal difference given by the following function:
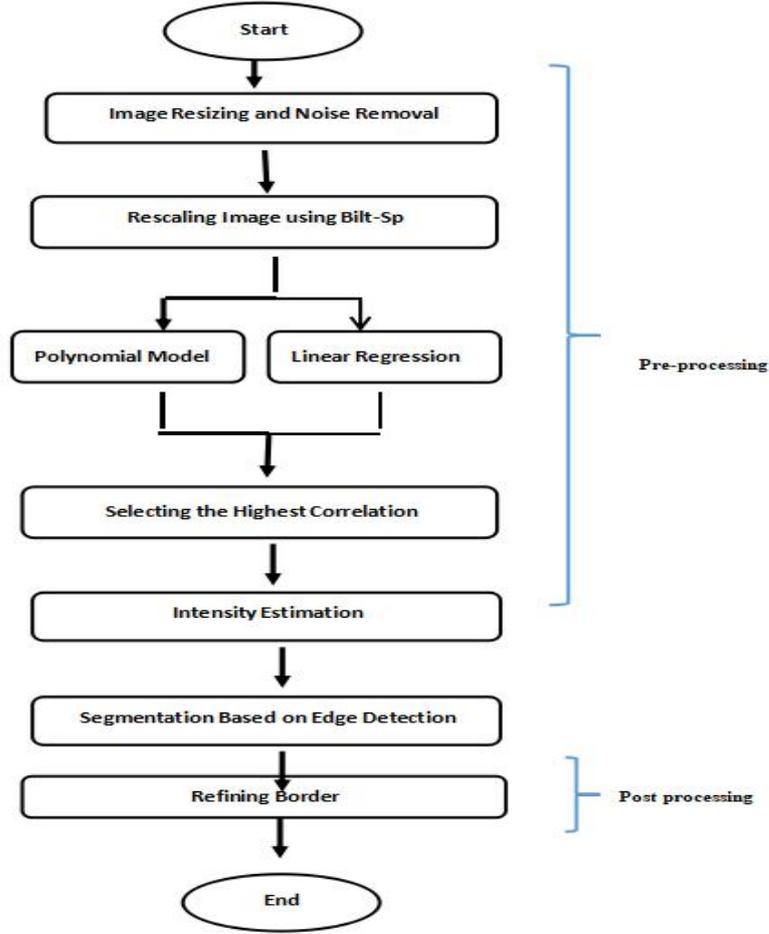
Figure 1. The flowchart of the proposed method with the solid line indicating the preferred steps (the dotted line shows tested techniques that were not used in the final implementation)

$$w(f(x) - f(y)) = \frac{1}{2} e^{-\frac{(f(x)-f(y))(f(x)-f(y))}{2\sigma^2_R}} \qquad (2)$$

where $f(.)$ denotes image intensity values or colour, and σ_R is the set of degree of tonal filtering.

$$\theta_k(i,j) = \frac{\int_{R^d} f(y)v(x-y)w(f(x)-f(y))\,dy}{\int_{R^d} v(x-y)w(f(x)-f(y))\,dy} \qquad (3)$$

where θ_k is the de-noised image, i and j represent the spatial coordinates of the image, and k indicates the colour channel (R, G or B).

It is difficult to compare the performance of de-noising algorithms on real world data without the ground truth. The Peak Signal-to-Noise Ratio (PSNR) was computed before and after adding noise by the following equations[6,9]:

The final formula of the bilateral filter is given below:

$$PSNR = 10 \log\left(\frac{MAX^2 (Q_k(i,j))}{MSE}\right) \qquad (4)$$

$$MSE = \frac{1}{MN} \sum_{i=1}^{M} \sum_{j=1}^{N} (Q_k(i,j) - x(i,j))^2 \qquad (5)$$

21

where x and Q_k *(i,j)* are the original noisy image and de-noised image with size $M \times N$, respectively, i and j represent the spatial coordinates of the images.

3.1.3 Intensity rescaling

Next, the smoothed image was rescaled to new intensities in order to improve edge detection on images with low contrast. The quality of edge detection was dependent on conditions such as lighting conditions among the objects of similar intensities, density of edges in the image, and noise. Each of these conditions could be handled by adjusting specific values of the edge around the object and changing the threshold value adaptively. The new image with improved contrast was

$$f_1(R_1(i,j),a,b) = \begin{cases} 0 & R_1(i,j) \leq a \\ 2\left(\frac{R_1(i,j)-a}{b-a}\right)^2 & a \leq R_1(i,j) \leq \frac{a+b}{2} \\ 1-2\left(\frac{R_1(i,j)+b}{b-a}\right)^2 & \frac{a+b}{2} \leq R_1(i,j) \leq b \\ 1 & R_1(i,j) \geq b \end{cases} \qquad (7)$$

where a and b are the slope of the curve which are

$$a = \min(R_1(i,j)) \qquad (8)$$

$$b = \frac{1}{mn}\sum_i^m \sum_j^n R_1(i,j) - c \qquad (9)$$

where c has the optimal value of 3 as calculated from our previous work[29]. The smoothing spline used in this

calculated by using the following equation[29]:

$$R_1(i,j) = Trans[\theta_k(i,j) * 0.25] \qquad (6)$$

where, $R_1(i,j)$ is the new image with improved contrast, *Trans* is the transformation using spline function, and k is the green colour channel.

3.1.4 Spline smoothing

The spline is a fuzzy set function that is named based on the shape of the function as letter (S) that was implemented to obtain smooth images for improving the segmentation results. The spline function is computed by the following equation[30]:

calculated in the following equations:

work minimized error ϵ_i that is calculated by the following formula:

$$\epsilon_i = \sum (\theta_k(i,j) - f_1(R_1(i,j),a,b))^2 \qquad (10)$$

3.1.5 Intensity estimation

Polynomial regression is a type of linear regression in which the relationship between the independent and dependent variables. Linear regression was calculated using the following equation[18]:

$$s = a_0 + a_1 R_1(i,j) \qquad (11)$$

Generally, polynomial model with second order equation is given by:

$$v(i,j) = b_0 + b_1 R_1(i,j) + b_2 R_1^2(i,j) \qquad (12)$$

where $b_0, b_1, b_2, \dots b_l$ are coefficients of the model.

The estimation intensity $\xi(i,j)$ was computed by the following formula:

$$\xi(i,j) = b_0 + b_1 v(i,j) + b_2 v^2(i,j) \qquad (13)$$

Data fitting was an important process as best fit implied minimizing the sum of squared residuals, which

was computed by finding the differences between the observed values and fitted value provided by a model.

3.2 Segmentation based on edge detection

Various types of edge detectors can be used to identify the border around a skin lesion. Edge detection is dependent on the knowledge of the image. The Prewitt edge detector computes an approximation of the gradient image. It replaces either the corresponding gradient vector or the norm of the vector at each pixel of an image. The Prewitt is based on convolving the image in horizontal and vertical direction. The Sobel edge detector has two convolution masks, horizontal and vertical, to approximate the gradient of the pixel at the centre of the masks. Zero-crossing detects edges through second order derivative by computing the differences

22

between negative and positive values. The Canny edge detector uses a multi-stage algorithm to detect a wide range of edges in images. It can be approximated by the first derivative of a Gaussian.

Generally, thresholding is used after applying the Sobel edge detector to detect the edges of lesion. In this case, low threshold would increase false negative detection but high threshold would lead to higher false positive detection[24]. Similar to Sobel edge detector, the Prewitt edge detector works very well but it is sensitive to noise. The zero-crossing technique has fixed characteristics in all directions in edge detection. In addition, it is sensitive to noise and involves complex computations. On the other hand, the Canny edge detector is adaptable to various environments[37]. Thus, it can be modified to solve problems such as contour. Moreover, it is more accurate than other edge detectors as it responses only to single edge[36,30].

3.3 Refining border and evaluation

The morphological operations as closing, thickening, and filling were implemented in order to fill the gaps in the borders and refine the border of the lesion. Finally In this research work, the segmentation results were evaluated using three metrics: sensitivity, specificity and accuracy. These metrics were calculated using following functions[24,30,33,34]:

$$Sensitivity = \frac{TP}{TP+FN} \times 100\% \qquad (14)$$

$$Specificity = \frac{TN}{TN+FP} \times 100\% \qquad (15)$$

$$Accuracy = \frac{TN+TP}{TP+TN+FN+FP} \times 100\% \qquad (16)$$

where *TP* is the number of overlapping pixels in the lesion, *TN* is the number of overlapping pixels outside the lesion, *FP* is the number of overlapping pixels between the automatically labelled lesion and those outside the manually labelled lesion, and *FN* is the number of overlapping pixels between the manually labelled lesion and those outside the automatically labelled lesion[31,24].

## 4. Experimental Results and Discussions

Evaluations were conducted to test several techniques at different stages in our method, as shown in **Figure 1**, and the techniques with the best performance were adopted in the proposed method to give the best segmentation result. After removing noises such as hair and lighting were effected using morphological operations at the pre-processing stage as shown in **Figure 2**.

Figure 2. Removal of hair (a) and lighting (b) from dermoscopy images.

In the image smoothing stage, four filter techniques were tested as average, median, Gaussian, and bilateral filters. PSNR was applied to select the optimal filter as shown the results in **Figure 3**. The bilateral filter has provide consistently the highest PSNR results amongst other filters.

After applying Spline for intensity smoothing, the linear regression model and second order polynomial model were tested separately to fit the smooth intensity of the image for intensity estimation.

23
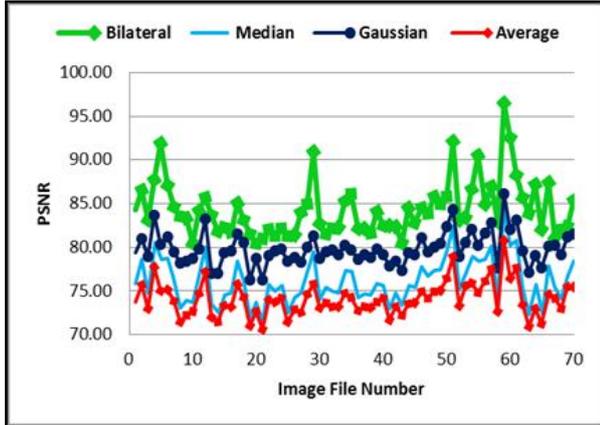
Figure 3. The results of comparison between the four filters. The highest PSNR is bilateral filter.

The second order polynomial model was selected as it has the higher correlation between both smooth and estimated intensities as shown in **Table 1**. It can be seen that by comparing the correlation results, the polynomial model produces a better correlation than the linear regression model for both grey and G-opt images. Between grey image and the G-opt image, the polynomial model estimation has a higher correlation in the latter case.

Table 1. The relationship between two models using the correlation based on BiltSp

Model Name	Grey Level	G-Opt
Second Order Polynomial Model	0.9739	0.9782
Linear Regression	0.7805	0.8555

To segment the skin lesion from the healthy skin area, we have implemented the Canny edge detector to facilitate segmentation. In comparison with other types of edge detection techniques, such as Canny, Zero-crossing, Prewitt and Sobel, which are more prone to be overly sensitive towards noise. In order to verify the segmentation performance of Canny edge detector, it was combined with the previously adopted techniques.

Three metrics were used to evaluate the effectiveness of the proposed method which was tested on a database of 70 clinical dermoscopic images. the performance of the Canny edge detector, three other edge detector techniques were also tested in the segmentation stage for comparison. As seen in **Figure 4**, the average

accuracy achieved by using the Canny edge detector was the highest for both grey level images as well as the green channel (G-Opt) intensity, with the best accuracy of 96.69% for the latter case. The average accuracy presented in our previous work had shown that the highest accuracy of 96.26% was achieved by a combination of the bilateral filter with Spline and Canny (Bilt-Sp)[35]. In this paper, the accuracy of segmentation was improved by adding an intensity estimation stage with second order polynomial model (BiltSp-Poly). As a result, the highest average accuracy attained was 96.69%.

Figure 4. Comparison the average segmentation accuracy based on proposed method BiltSp-Poly using different edge detectors.

5. Conclusion

This paper has proposed an enhanced method for skin lesion segmentation using a combination of techniques that has shown good results when compared with similar techniques. The adopted method, includes bilateral filter for image smoothing, then Spine was implemented for intensity smoothing, the second order polynomial model was then used for intensity estimation, before applying the Canny edge detector for skin lesion segmentation. Satisfactory result was obtained when the proposed method was applied on a set of 70 clinical dermoscopic images from different sources.

In the future, we propose to extend our segmentation method using more complex mathematical techniques as well as expanding to other types of lesions.

Acknowledgment

References

1. Jaleel JA, Salim S, Aswin RB. Artificial neural network based detection of skin cancer. International Journal of Advanced Research in Electrical, Electronics and Instrumentation Engineering 2012; 1(3): 200-205.

2. Ahmad MB, Choi TS. Local threshold and boolean function based edge detection. Consumer Electronics, IEEE Transactions on 1999; 45(3): 674-679.

3. Stoecker WV, Gupta K, Stanley RJ, et al. Detection of asymmetric blotches (asymmetric structureless areas) in dermoscopy images of malignant melanoma using relative color. Skin Research and Technology 2005; 11(3): 179-184.

4. Celebi ME, Kingravi HA, Aslandogan YA, et al. Detection of blue-white veil areas in dermoscopy images using machine learning techniques. In Medical Imaging, International Society for Optics and Photonics 2006; pp: 61445T-61445T.

5. Tomasi C, Manduchi R. Bilateral filtering for gray and color images. In Computer Vision, Sixth International Conference, IEEE 1998; pp: 839-846.

6. Francis JJ, De Jager G. The bilateral median filter. In Proceedings of the 14th Symposium of the Pattern Recognition Association of South Africa 2003.(Pires & Barcelos, 2007)Manfred Kudlek, Yurii Rogozhin. A universal turing machine with 22 states and 2 symbols. Romanian Journal of Information Science and Technology 1998; 1(3): 259‑265.

7. Hu Q, He X, Zhou J. Multi-scale edge detection with bilateral filtering in spiral architecture. In Proceedings of the Pan-Sydney Area Workshop on Visual Information Processing, Australian Computer Society, Inc 2004; pp: 29-32.

8. Pires VB, Barcelos CAZ. Edge detection of skin lesions using anisotropic diffusion. In Intelligent Systems Design and Applications, ISDA, Seventh International Conference, IEEE 2007; pp: 363-370.

9. Chiu LC, Fuh CS. A robust denoising filter with adaptive edge preservation. In Advances in Multimedia Information Processing-PCM, Springer Berlin Heidelberg 2008; pp: 923-926.

10. Sameh Arif A, Mansor S, Logeswaran R. (2011, December). Combined bilateral and anisotropic-diffusion filters for medical image de-noising. In Research and Development (SCOReD), IEEE Student Conference, IEEE 2011; pp: 420-424.

11. Garnavi R, Aldeen M, Bailey J. Computer-aided diagnosis of melanoma using border and wavelet-based texture analysis. IEEE Transactions on Information Technology in Biomedicine A Publication of the IEEE Engineering in Medicine & Biology Society 2012.

12. Yasmin JJ, Sathik MM. Skin Lesion Segmentation Algorithms using Edge Detectors. International Journal of Computer Science & Information Security.

13. Bhonsle D, Chandra V, Sinha GR. Medical image denoising using bilateral filter. International Journal of Image, Graphics and Signal Processing (IJIGSP) 2012; 4(6): 36.

14. Mahmoud MKA, Al-Jumaily A, Takruri M. The automatic identification of melanoma by wavelet and curvelet analysis: Study based on neural network classification. In Hybrid Intelligent Systems (HIS), 11th International Conference, IEEE 2011; pp: 680-685.

15. Liu D, Xiong Y, Pulli K, et al. Estimating image segmentation difficulty. Proceedings of the 7th International Conference on Machine Learning and Data Mining in Pattern Recognition (MLDM'11), Petra Perner (Ed.), Springer-Verlag, Berlin, Heidelberg 2011; pp: 484-495.

16. Nagi Zomrawi Mohammed, EimanEisa Ahmed Elhaj. The effect of polynomial order on georeferencing remote sensing images. International Journal of Engineering and Innovative Technology (IJEIT) 2013; 2(8): 5-8.

17. Hani AFM, Prakasa E, Fitriyah H, et al. High order polynomial surface fitting for measuring roughness of psoriasis lesion. In Visual Informatics: Sustaining Research and Innovations, Springer Berlin Heidelberg 2011; pp: 341-351.

18. Almedeij J. Modeling pan evaporation for kuwait by multiple linear regression. The Scientific World Journal 2012.

19. [19] Celebi ME, Iyatomi H, Schaefer G, et al. Lesion border detection in dermoscopy images. Computerized Medical Imaging and Graphics 2009; 33(2): 148-153.

20. [20] Garnavi R, Aldeen M. Optimized weighted performance index for objective evaluation of border-detection methods in dermoscopy images. Information Technology in Biomedicine, IEEE Transactions 2011; 15(6): 908-917.

21. Iyatomi H, Oka H, Saito M, et al. Quantitative assessment of tumour extraction from dermoscopy images and evaluation of computer-based extraction methods for an automatic melanoma diagnostic system. Melanoma Research 2006; 16(2): 183-190.

22. Emre Celebi M, Alp Aslandogan Y, Stoecker WV, et al. Unsupervised border detection in dermoscopy images. Skin Research and Technology 2007; 13(4): 454-462.

23. Garnavi R, Aldeen M, Celebi ME, et al. Automatic segmentation of dermoscopy images using

histogram thresholding on optimal color channels. International Journal of Medicine and Medical Sciences 2010; 1(2): 126-134.

24. Garnavi R, Aldeen M, Celebi ME, et al. Border detection in dermoscopy images using hybrid thresholding on optimized color channels. Computerized Medical Imaging and Graphics 2011; 35(2): 105-115.

25. Viana JMDC. Classification of skin tumours through the analysis of unconstrained images 2009.

26. Abbas AA, Guo XN, Tan WH. An improved automatic segmentation skin lesion from dermoscopic images using optimal RGB channel. Proceedings of the 2nd International Conference on Computer Science & Computational Mathematics, Kaula Lumpur, Malaysia 2013.

27. Maini R, Aggarwal H. Study and comparison of various image edge detection techniques. International Journal of Image Processing 2009; 3(1): 1-11.

28. Eubank RL. Nonparametric regression and spline smoothing. CRC press 1999.

29. Sadeghi M, Razmara M, Lee TK, et al. A novel method for detection of pigment network in dermoscopic images using graphs. Computerized Medical Imaging and Graphics 2011; 35(2): 137-143.

30. Razmjooy N, Mousavi BS, Soleymani F, et al. A computer-aided diagnosis system for malignant melanomas. Neural Computing and Applications 2013; pp: 1-13.

31. Abbas AA, Tan WH, Guo XN. Combined optimal wavelet filters with morphological watershed transform for the segmentation of dermoscopic skin lesions. Pacific Rim International Conference on Trends in Artificial Intelligence 2012; 7458: 722-727. Addison JW, Moschovakis YN. Some consequences of the axiom of definable determinanteness. Proc. Acad. Sci. U.S.A. 1967; 59: 708-712.

32. He Y, Xie F. Automatic skin lesion segmentation based on texture analysis and supervised learning. In Computer Vision – ACCV, Springer Berlin Heidelberg 2012; pp: 330-341.

33. [35] Abbas AA, Logeswaran R, Guo XN, et al. Lesion border detection in dermoscopy images using bilateral filter. IEEE International Conference Signal Processing and Applications 2013.

34. Heath M, Sarkar S, Sanocki T, et al. Comparison of edge detectors: A methodology and initial study. In Computer Vision and Pattern Recognition, Proceedings CVPR'96, IEEE Computer Society Conference 1996; pp: 143-148.

35. Gao W, Zhang X, Yang L, et al. An improved sobel edge detection. In Computer Science and Information Technology (ICCSIT), 3rd IEEE International Conference 2010; (5): 67-71.

36. Ziou D, Tabbone S. Edge detection techniques-An overview. International Journal of Pattern Recognition & Image Analysis 1998; 8: 537-559.

37. Zhao Y, Gui W, Chen Z. Edge detection based on multi-structure elements morphology. In Intelligent Control and Automation, WCICA, The Sixth World Congress, IEEE 2006; (2): 9795-9798.